TECHNICAL PAPER

Development of a trigger mechanism with circular cut-outs to improve crashworthiness characteristics of glass fiber-reinforced composite pipes

Özkan Özbek[1] · Ömer Yavuz Bozkurt[2] · Ahmet Erkliğ[2]

Abstract

The present work is concerned with the improvement of crashworthiness characteristics of glass fiber-reinforced composite pipes (GFRP) by developing a trigger mechanism through circular cut-outs. To induce progressive crushing of the GFRP samples, circular cut-outs with varied geometrical designs in terms of number, position, and diameter were used. The wet filament winding process was used to fabricate the GFRP samples with $\pm(55°)_6$ fiber orientation, which were then subjected to quasi-static axial compression test. The influence of cut-outs on the stability and fracture characteristics in a crash event was studied by analyzing the crashworthiness parameters such as load–displacement response, failure modes, crushing load efficiency, and energy absorption. Overall, the best performance for GFRP subjected to axial crushing was achieved from the samples having three cut-outs with the size of 10 mm diameters which are placed near to the impacted end.

Keywords Crashworthiness · Composite pipe · Circular cut-out · Trigger mechanism

1 Introduction

Safety in vehicles has become an increasingly important crucial phenomenon to prevent the occurrence of traffic accidents and minimize their consequences in terms of injuries and deaths. Nevertheless, even if adequate precautions are taken, accidents resulted with death or injury are occurred due to human errors or unexpected situations. In 2018, World Health Organization (WHO) has reported that around 3700 people per day (approximately 1.35 million each year) lose their lives in road accidents which are recorded as the first death reason for children and young adults [1]. Since the early 1960s [2], there have been several international regulations for the vehicle safety, consisting of important criteria such as lighting, crashworthiness, environmental protection, theft prevention and are strictly controlled by specialized companies before being made available to customers. Among those, crashworthiness regulations, also known as frontal, rear and side impact, are one of the most critical standards that recommend materials with a high crushing feature in terms of energy absorption, crushing load efficiency and failure modes in the case of unforeseen traffic accidents.

A crumple zone, which is called a crash box, in a vehicle is a necessity for intending the energy absorption and protecting the longitudinal members of the vehicles [2]. In a vehicle collision, the crash box collapsing before being deformed of system components behind it, absorbing energy and minimum damage to the whole vehicle and ensuring the passenger safety, should be designed as carefully as possible. The crashworthiness of the material used in the crash box has great importance depended on not only for intrinsic properties of materials but also geometry and design perspectives. Thus, the requirements in the vehicle design against unavoidable crash events to minimize the casualties must be satisfied by using optimum material in terms of geometry, weight, and mechanical response. Nowadays, geometrical modifications or triggering mechanisms ruling the material damage process with reducing the peak load at acceptable energy absorption levels are investigated for a

---

✉ Özkan Özbek
  ozkanozbek@kilis.edu.tr

1 Faculty of Engineering and Architecture, Mechanical Engineering Department, Kilis 7 Aralık University, 79000 Kilis, Turkey

2 Faculty of Engineering, Mechanical Engineering Department, Gaziantep University, 27310 Gaziantep, Turkey

stable progressive crush process with increasing crushing load efficiency instead of the catastrophic failures [3]. The implementations of geometric modifications, as a means of controlling the crushing process in order to limit the forces acting on the passengers by reducing accelerations and to provide a survivable volume, are getting the attention of researchers. The geometrical modifications in various forms such as hole [4, 5], chamfer [6–8], steeple [9, 10], plug [11, 12], ply-drop-off [13, 14], tulip [16] to obtain a trigger mechanism are popularly seen in the literature. Among those, with their easy machining, holes or cut-outs are the most widely used forms in engineering applications. Kafer et al. [17] performed experimental and numerical studies on the effects of cut-out position and cut-out lengths on the crashworthiness of aluminum tubes. The circumferential notches were introduced on the top side of the tube samples, and it was shown that an increase in the lengths of notch position exhibiting high crushing efficiency resulted in the change of deformation modes from mixed to 3-lobe diamond folding. Chiu and Jenq [18] conducted a numerical study on the crashworthy of metallic thin-wall tubes with hole triggering mechanisms. The aluminum square samples with different cut-outs (circular, elliptical, and slotted) at the middle portion were analyzed by LS-DYNA finite element solver. A decrease of 11.7% in the initial peak load was reported for 4.3 mm circular cut-out samples. Rai et al. [19] carried out a comparative study on various trigger mechanisms (cut-outs, end filets, circumferential notches) to provide better crush force efficiency of aluminum tubes. It was shown that the samples with cut-outs exhibiting a 104% increase in crush force efficiency provided the best crushing performance. Very stable crush processes ensuring progressive collapses were obtained from the samples having trigger mechanisms.

Recently, manufacturers are encouraged to use composites rather than classical metal-based materials in the design of vehicles [20] to meet the crashworthiness requirements and to reduce fuel consumption [21]. The polymer-based composites providing superior mechanical properties such as higher specific strength/stiffness, longer fatigue life, better corrosion resistance [22–32] have been a promising alternative materials for metals in view of weight-saving and crash loadings [19]. They also facilitate high level of energy dissipation which are suitable for crash structures [33] due to their complex failure modes such as lamina bending, transverse shearing, brittle fracture, and buckling [34–36]. Many studies devoted to the crashworthiness of polymer matrix composites can be seen in the literature [37–42]. Liu et al. [43] performed a study related to the crushing characteristics of double hat-shaped carbon fiber-reinforced composites. The samples with three different numbers of layers as 3, 6, and 9 were subjected to loadings of the quasi-static axial compression and transverse bending. It was reported that thickness has significant influences on failure mechanisms

and the energy absorption capability of samples. Hu et al. [44] examined the effect of fiber orientation on the crashworthiness of glass cloth/epoxy fiber-reinforced composite tubes subjected to quasi-static and impact loadings. They stated that the energy absorption capability of the samples exposing to impact was found to be slightly lower than the sample results obtained from quasi-static axial compression.

Even though composite materials are a good choice for crushing applications, sometimes they suffer from catastrophic failures that lead to an increase in acceleration experienced by occupants in a vehicle. Thus, further researches must be devoted to trigger mechanisms or geometrical modification for development of better designs with polymer composites. Although there are some scientific studies about trigger mechanisms on the crushing behaviors of composites, it has still a big gap in the literature and should be supported with novel researches. Sivagurunathan et al. [45] investigated the effects of trigger mechanisms on the crushing behaviors of jute fiber-reinforced composites. All triggered tube samples exhibiting the stable progressive failure modes showed better crushing properties compared to nontriggered samples. Overall, the tulip type of trigger mechanism had the highest energy absorption capability. Jimenez et al. [46] conducted an experimental study to explore the effect of trigger geometry on the pultruded glass/polyester fiber-reinforced profiles. Two different samples having an I-section and a box section were prepared with six different trigger mechanisms. Bevel triggers depending on the bevel angle showed the best energy absorption. Song et al. [47] performed a study to improve the crashworthiness of square carbon fiber-reinforced composites with the implementation of cut-out and chamfers. It was reported that the optimum results were achieved from the samples having a cut-out and 45° chamfer exhibiting the progressive crushing mode.

It is seen that the studies on the literature mainly aim at evaluating the effects of trigger mechanisms on the crashworthiness of the composite pipes. Even though a great number of studies related to the trigger mechanisms on the energy absorption characteristics of the metal-based pipe-like structures are found, limited studies have been devoted to the influence of trigger mechanisms on the energy absorption characteristics of the composite pipes. Furthermore, it is not encountered with a study related to the influence of circular cut-outs on the crashworthiness performance of filament wound composite pipes. To this end, the influence of circular cut-outs on the crashworthiness performance of GFRP has been comprehensively examined for the first time in the literature with this study. By considering its widespread use in engineering applications due to its easier machining process compared to other geometries, it is focused on only circular shape for cut-outs in this study. The GFRP samples with $\pm(55°)_6$ fiber orientation were fabricated by the wet filament winding technique and subjected

to quasi-static axial compression loading. The GFRP pipe samples were firstly grouped into three categories. In the first group, various numbers of circular cut-outs (0, 2, 3, and 4) at the middle portion of pipe samples were drilled to assess the effect of number of circular cut-outs. In the second group, from mid to top portion of samples, circular cut-outs were introduced to four different locations, respectively, to analyze the influence of cut-out locations. In the third group, circular cut-outs which were different in diameters (6, 8, 10, 12 and 14 mm) for each sample were drilled to evaluate the effect of diameter values on crushing behavior. The crush characteristics of these three groups were comparatively examined to detail understand the effects of circular cut-outs on fracture characteristics of GFRP samples.

2 Materials and method

2.1 Materials

Glass roving fiber supplied from Plasto A.Ş., Turkey, was used as the reinforcement material to evaluate the crash-worthiness of filament wound composite pipes. Due to their high compatibility with glass fiber, a mixture of an epoxy (EPIKOTE MGS L160) and a hardener (EPIKURE Curing Agent MGS H260S) obtained from Dost Kimya A., Turkey, were selected for the production of the matrix phase. The epoxy, exhibiting a density ranging from 1.13 to 1.17 g/cm^3, and viscosity from 700 to 900 mPas at 25 °C and hardener having a density and viscosity from 0.96 to 1.00 g/cm^3, 10 to 50 mPas at 25 °C, were mixed with the stoichiometric weight ratio of 100:36, respectively. The mixing process was conducted by using a mechanical stirrer at 8000 rpm until no clouding is visible that approximately takes 30 min. Table 1 shows the mechanical and physical properties of raw materials.

2.2 Preparation of samples

Tubular samples with circular cross sections were used to facilitate crushing tests because they absorb more energy and prevent stress concentrations as a result of a more progressive crushing process than square or rectangular samples [33, 46, 48]. Wet filament winding was used to create GFRP pipes with a length of 450 mm, which is one of the

most efficient ways for producing hollow cross-sectional components [49]. A bundle of glass direct roving fiber comprising of only one strand with 3.8 mm bandwidth was impregnated with unsaturated epoxy resin and wrapped around the mandrel. To assure the same material, the same fabrication method was used on a total of 12 pipes for each design parameter. Then, GFRP pipes were cut using diamond sawing to provide a flat cross section. Finally, a CNC milling machine was used to drill circular cut-outs in each pipe sample. The production flow of GFRP pipe samples is shown in Fig. 1.

As shown in Fig. 2, three design parameters were used to examine the best design configuration of circular cut-outs. First, the influence of surface discontinuities on the damage and crushing properties of GFRP pipes was investigated using a variety of cut-outs. In order to evaluate the effect of the number of cut-outs, 10-mm diameter holes were drilled in the center of the GFRP samples, and each configuration was compared with the samples without cut-out. After deciding on the number of cut-outs to drill, the application of holes at different places was considered, with the goal of contributing to the crushing process by lowering the first peak load, i.e., increasing crush load efficiency. As a result, the cut-out location at four different regions as C, M2, M1, and T was examined to investigate the crushing load stability on load–displacement diagrams in view of reducing accelerations experienced by passengers. Finally, the size of cut-outs (4, 6, 8, 10, 12, and 14 mm) was investigated in order to determine the best configuration in examined crashworthiness parameters.

The GFRP samples, which had the identical dimensions, i.e., their length, inner diameter, and thickness were 72 ± 0.5 mm, 46.3 ± 0.2 mm, and 4.75 ± 0.1 mm, respectively, were prepared using very precisely sawing machines. Fiber mass fractions of GFRP samples were determined by ignition loss experiments according to the ASTM D2584 standard [50]. The samples were kept at 650 °C temperature for 1.5 h in a high-capacity furnace until disappearance of the cured epoxy matrix in order to determine fiber mass fractions. After that, the weight of the remaining part, which was the fiber reinforcements, was measured and divided by initial weight of the samples. Finally, fiber mass fractions were found as 55% within the tolerance of ± 0.34. At least four numbers of GFRP samples were employed for each design parameter to ensure experimental reliability in the results.

Table 1 The mechanical and physical properties of raw materials

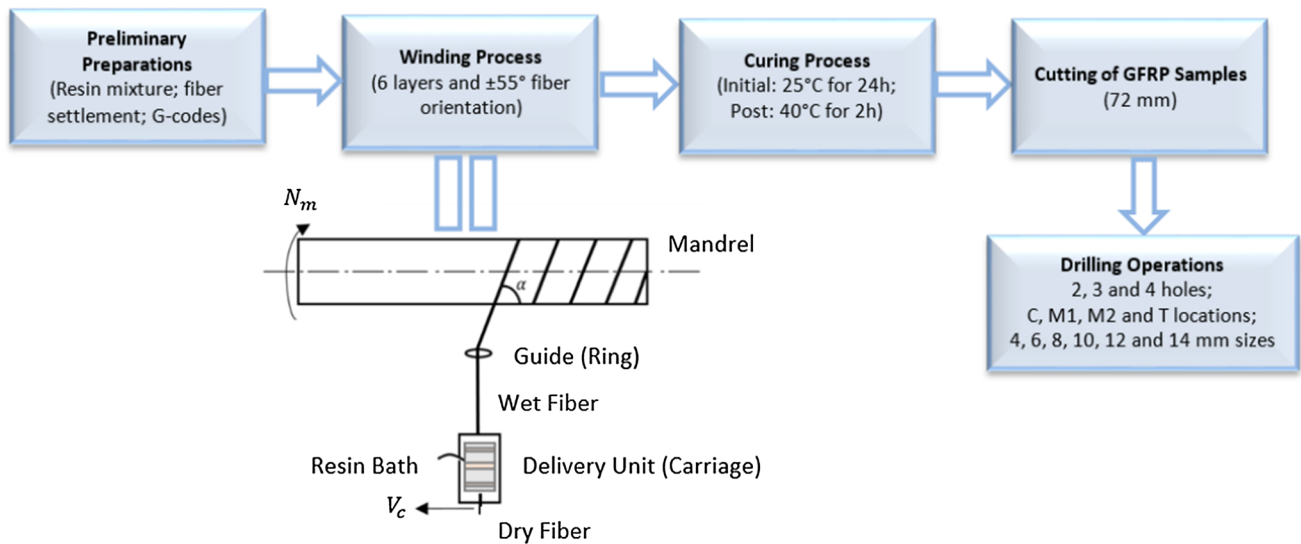| Fiber material	Linear density (tex)	Tensile strength (MPa)	Tensile modulus (GPa)	Elongation at break (%)	Filament diameter (μm)	Specific density (g/cm^3)
Glass fiber	2.4 K	1970	79	3.5	17	2.56
Neat epoxy	–	70–80	3.2–3.5	5.0–6.5	–	1.18–1.20

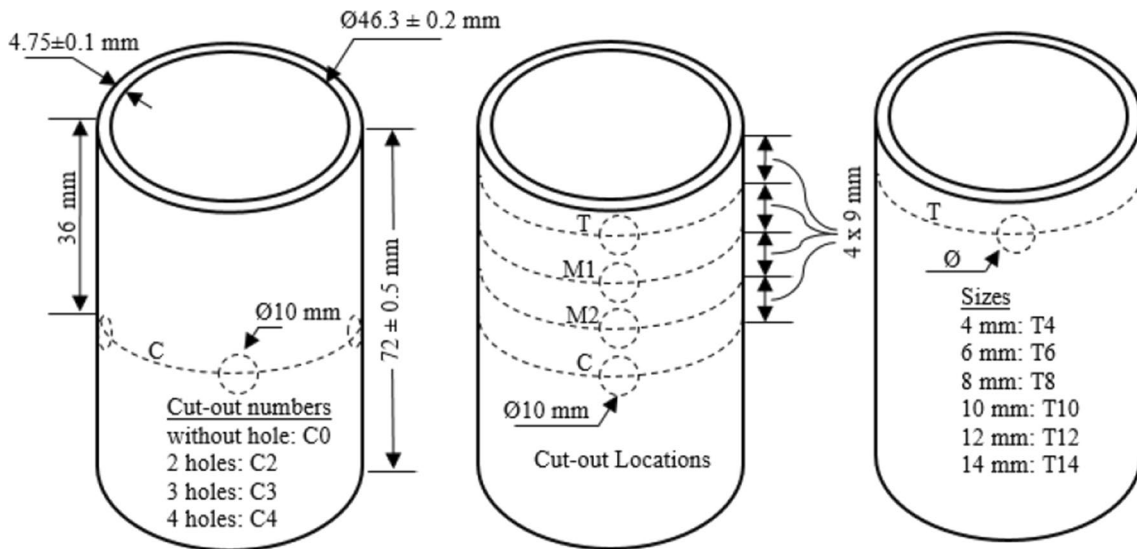**Fig. 1** Production flow of GFRP test samples

Fig. 2 Naming and geometry of the designed GFRP samples

2.3 Quasi-static axial compression tests

For the determination of crashworthiness behaviors, the GFRP samples were subjected to quasi-static axial compression loadings on a universal testing machine with a frame capacity of 300 kN (Shimadzu AG–X Series) as depicted in Fig. 3. The pipe samples between two steel plates (moving and stationary) loaded at a constant cross-head speed of 5 mm/min were axially compressed up to 80% stroke efficiency (57.6 mm in stroke). After this point, the compression process was stopped due to a sharp increase in load values that called as beginning of the densification phase. Then, the crushing load and displacement information were recorded

by an automatic data acquisition system. By the way, photographs at different stroke values in crushing samples were taken by a camera to understand the failure characteristics of entire the crash application.

In general, the load–displacement curve of the brittle materials like composites subjected to crushing experiments can be divided into three main stages as pre-crushing, post-crushing, and material densification as shown in Fig. 4. The pre-crushing stage, which represents the elastic region, that material can be returned to its original length if the applied load is removed, is directly related to the protection of the passengers. Because it plays a significant influence in crushing load efficiency, the initial
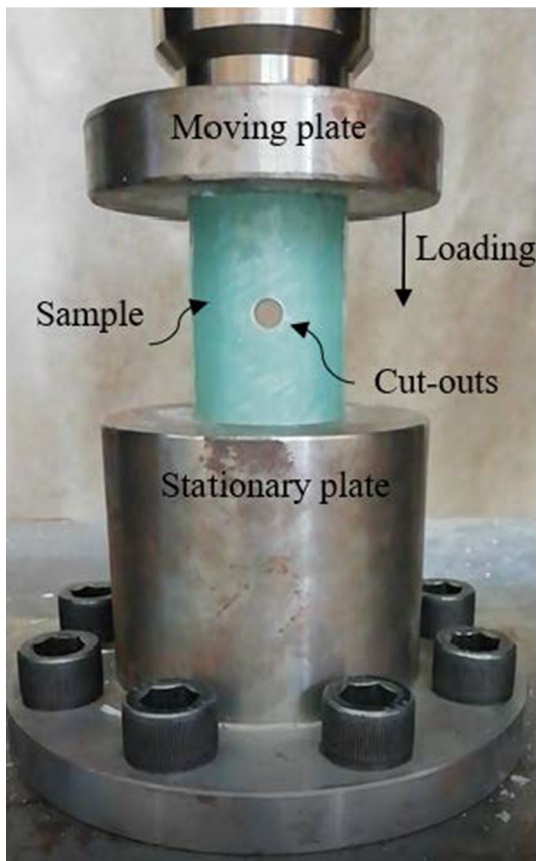
Fig. 3 Quasi-static axial compression test

peak load is the only important characteristic for crushing applications. Following the first peak load point, the

post-crushing stage begins with small inter- or intralaminar cracks nucleating with local stress concentrations, which is the most crucial for measuring and understanding the crashworthiness characteristics of samples. At last, material densification, which represents the almost complete compaction of the compressed sample, is happened due to the sharp increases in load.

The crashworthiness parameters of the samples such as total energy absorption, mean crushing load, crushing load efficiency, and specific energy absorption can be calculated as follows [51]:

Total energy absorption, E, represents the area under the curve of the load in crushing vs displacement in moving plate, as given in Fig. 4, is calculated by integration of load, P as in Eq. (1);

$$E = \int_{S_i}^{S_f} P(s)ds \tag{1}$$

where S_i and S_f represent the initial and final stroke values in the post-crushing stage. Also, the mean crushing load, P_m, obtained from the integration of each load depending on sample length is calculated with Eq. (2);

$$P_m = \frac{\int_{S_i}^{S_f} P(s)ds}{S_f} \tag{2}$$

Crushing load efficiency, η_f, which is a measurement parameter for understanding the stability of the crushing process and absorption performance of the samples, is found from the mean crushing load per initial peak load and is calculated as shown in Eq. (3);

Fig. 4 The typical load–displacement response curve of the crushing experiments [35]
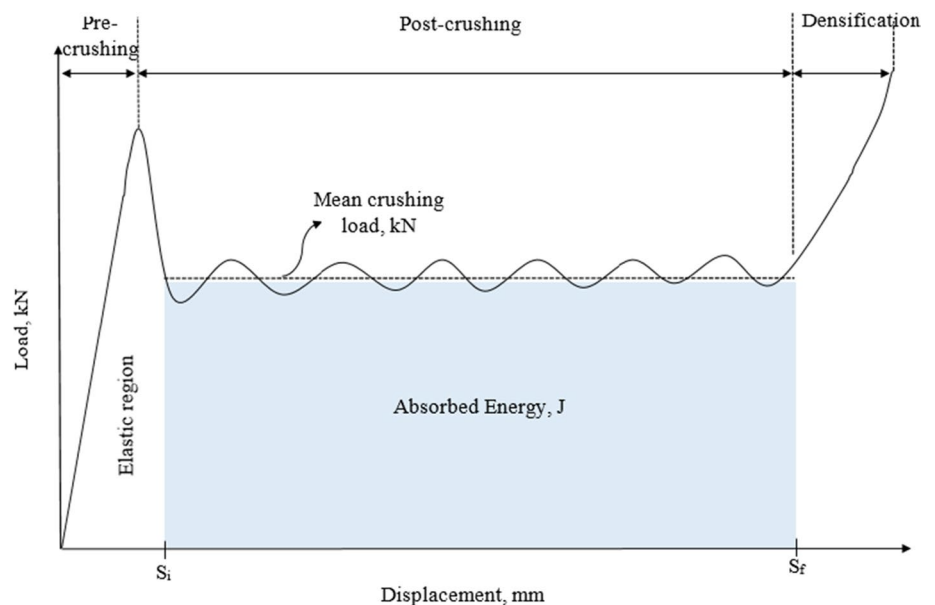
$$\eta_f = 100 \frac{P_m}{P_i} \qquad (3)$$

where P_i is the initial peak load which is commonly the maximum load in a crushing process.

Specific energy absorption, E_s, which is the most important parameter to understand material performance under compressive loads, is the absorbed energy per mass of the crushed sample as shown in Eq. (4);

$$E_s = \frac{E}{m_{crush}} = \frac{\int_{S_i}^{S_f} P(s)ds}{m_{crush}} \qquad (4)$$

3 Results and discussion

3.1 Number of cut-outs

At first, pipe samples with four different numbers of cut-out configurations (0, 2, 3, and 4) at the middle portion were utilized to determine the contribution of the number of cut-outs on crush performance. Due to the asymmetric nature of cylindrical pipes, a single hole that resulted with an unstable crushing process did not considered [19]. As shown from Fig. 5a which represents the curves for the different numbers of cut-outs, all samples exhibited sharp decreases in load after the initial peak point [52]. Although C0 exhibited the maximum load-bearing capability in the elastic region and a closer curve for an ideal crushing process, it had the worst energy absorption and crushing load efficiency since damages begun at all middle sides causing the pipe samples to split and fracture into several separated segments [5]. Here, C3 samples (3 cut-outs) showing the highest energy absorption as a result of high crushing load efficiency were thought to be the best ones. The crushing histories for pipe samples are presented in Fig. 5b. While C0 samples showed the catastrophic drop at the middle portion, other samples exhibited parallel-to-fiber cracks due to the high-stress concentrations around the cut-outs. As seen from the figures, the cracks were begun to form near the holes and then exhibited a parallel propagation to fiber alignment according to winding angle [53]. This propagation resulted in the diamond shape failures [19], especially seen for C3 and C4 samples. The pipe samples after the crushing application are shown in Fig. 5c. The inner or outer frond formation was observed for all samples. Also, splaying characteristics for the fiber reinforcements were obtained from C0 samples. The matrix cracking, fiber debonding, and fiber breakages can be said as common failure modes for all samples. Similar findings devoted to the selection of the optimum number of cut-outs can be found in the literature. Rai et al. [19], who studied the development trigger mechanisms of aluminum tubes,

declared that the use of 3 circumferential cut-outs was the optimum one since the very stable collapse mode was observed from that compared to other numbers of cut-outs. Additionally, Zhang et al. [54] explained that the samples with 3 lobe numbers exhibiting the diamond mode failures showed a more stable deformation.

The loading characteristics of GFRP samples having several numbers of cut-outs are given in Fig. 6. To reduce accelerations experienced by occupants or to get minimum casualties in a vehicle crushing [19], the initial peak load and mean crushing load should be closer as possible which means higher crushing load efficiency. The difference between initial peak and mean crushing loads was showed a reduction for C2 and C3 samples and became minimum for C3 which showed higher crushing load efficiency, as 74.05%, compared to other ones. C3 exhibited the mean crushing load of 46.37 kN which was 20%, 3.26%, and 28.7% higher than C0, C2, and C4 samples, respectively. Furthermore, it was evident that the C0 sample with 75.21 kN initial peak load was the best for the application concerning only the elastic region, but it had the lowest crushing load efficiency (51.36%) that was explained by the most destructive failures as seen. This result was consistent with the study of Sivagurunathan et al.'s study [44] that declares the lowest crushing load efficiency was obtained from the composite tube samples without trigger mechanisms.

The effect of cut-out numbers on the energy absorption of the GFRP samples is presented in Fig. 7. C3 samples exhibiting 2546.6 J value showed the highest energy absorption which was 21.15%, 3.57%, and 28.9% more than the C0, C2, and C4 samples, respectively. This can be attributed to failure performance during the crushing process and the loading characteristics resulted in a higher area under the curve. Additionally, from the specific energy absorption results, C3 samples showed the 38.07 J/g specific energy absorption which means the 1.2, 1.035, and 1.26 times of that of C0, C2, and C4 samples, respectively. Here, the worst energy absorption characteristics in both the total and specific manner were obtained from C4 samples. It can be said that the decreasing tendency was started after a certain decrease in inertia. In conclusion, the pipe samples having 3 circular cut-outs were chosen as the best configuration in terms of the indicators of the failure response, loading characteristics, and energy absorption for the first group that deals with the number of circular cut-outs. Several studies devoted to the energy absorption of the materials that can be improved by trigger mechanisms are seen in the literature [7, 9, 12].

3.2 Location of cut-outs

After examination the number of cut-outs, the next step was the analyze of the effect of their locations on the crashworthiness. To this aim, four different regions were
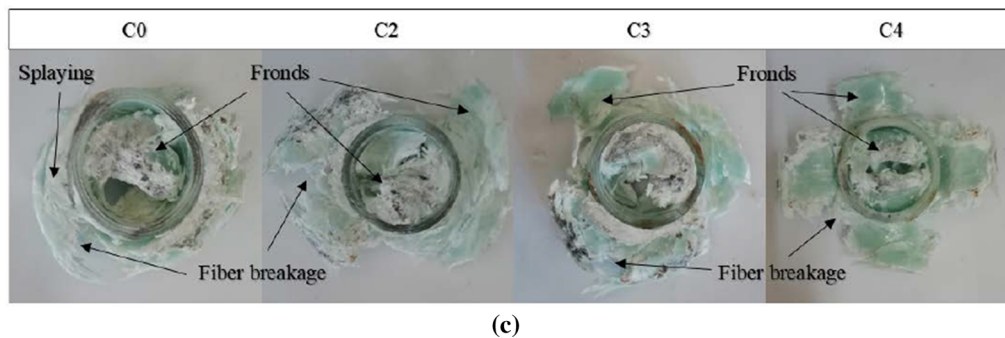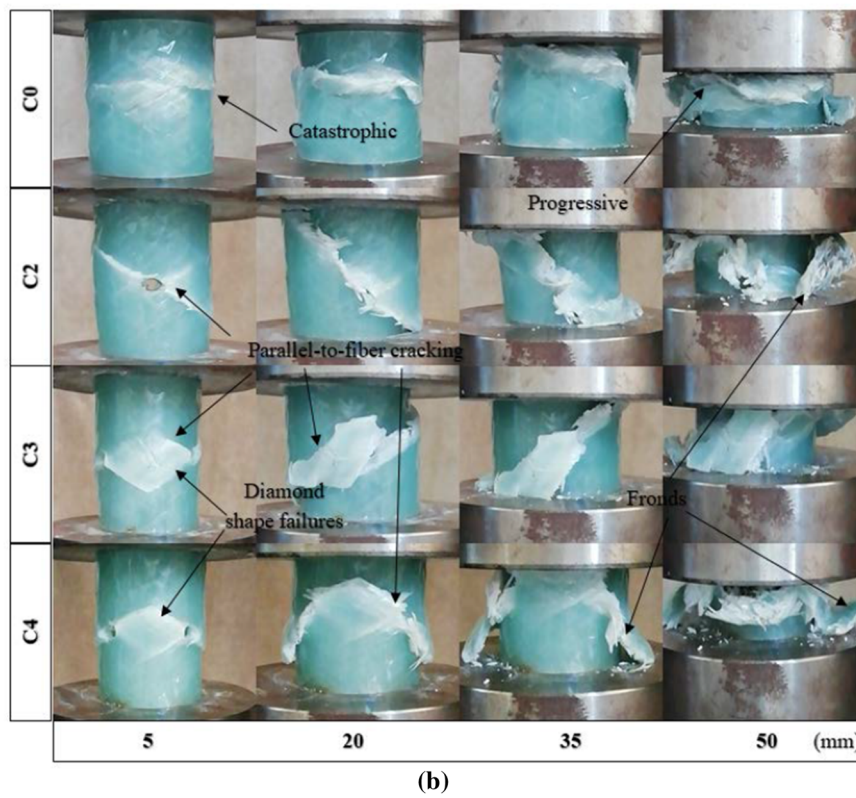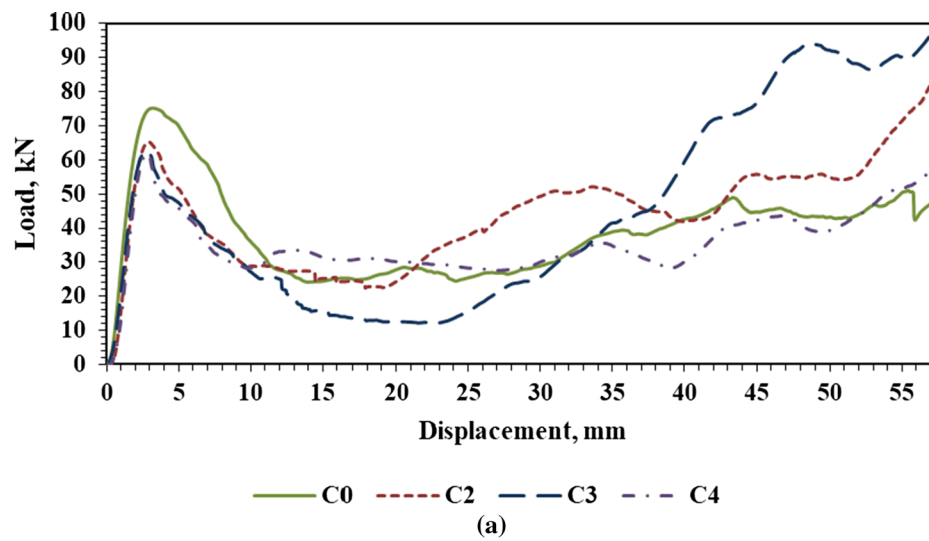
(a)

(b)

(c)

Fig. 5 GFRP samples with different numbers of cut-outs; **a** load–displacement response, **b** crush history, **c** after experiments
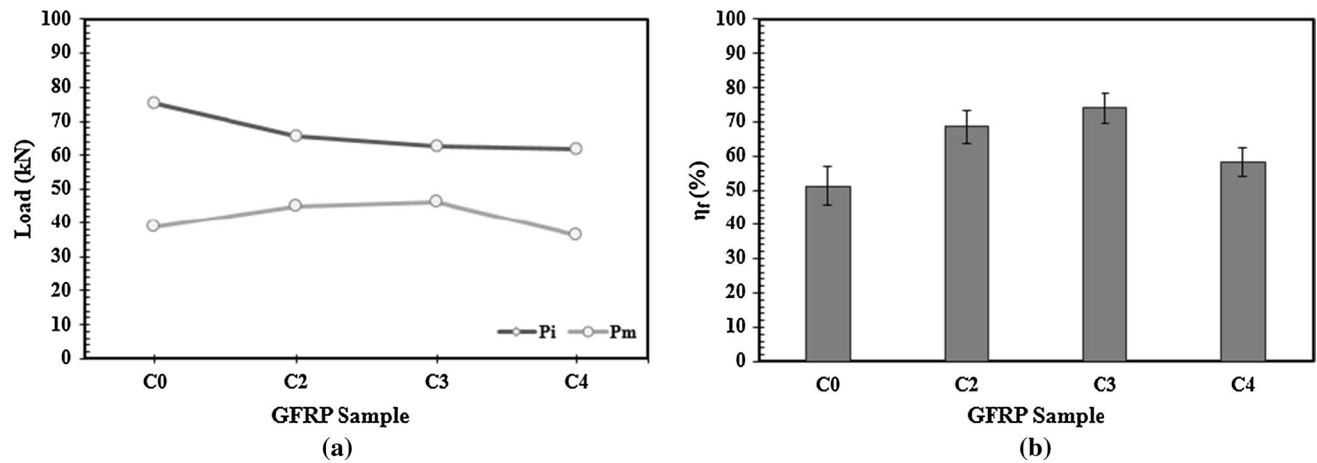
Fig. 6 Loading characteristics for different numbers of cut-outs; a) initial peak and mean loads, b) crushing load efficiency
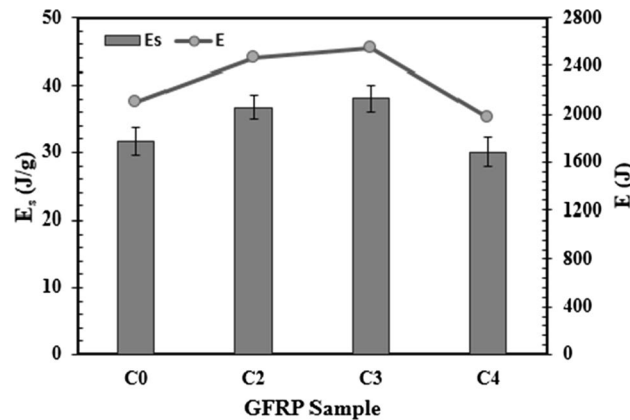

Fig. 7 Energy absorption for different numbers of cut-outs

considered from the middle part to the top end which is the loading side. Figure 8 represents the load–displacement curves, crushing history, and crushed samples, respectively. T samples exhibiting the most stable curve response showed the progressive crushing process. The parallel-to-fiber cracking failures were seen due to high-stress concentrations around the cut-outs [53]. Although all samples showed a drastic decrease in load after the initial peak, T samples fixing unstable crushing answered an earlier response for a higher crushing efficiency. The increased load in the crushing part was directly attributed to the blockage of compacted debris which acts as resistance. Also, splaying formations, especially for T samples, were seen entire the crushing process because the distance between cut-out regions to the end of the pipe was very short resulted in the easy rupture which activated the triggering that propagates the damage progressively throughout the sample [5]. Additionally, frond formations in both the inner and outer regions for all samples were observed. The energy absorption was attributed to

lamina bending and axial cracks for GFRP samples. Rai et al. [19] explained that the closer cut-outs to the impact end resulted in decreases in the initial peak load due to the compressive stresses on the cylinder as a result of the movement of the top end of the pipe to the inward to initiate the folding.

The initial peak and the mean crushing load values of the GFRP samples with circular cut-outs at various locations are shown in Fig. 9a. The maximum load-bearing capability or initial peak load value as 71.11 kN was obtained from T samples, while the minimum one was 62.62 kN of C samples. Furthermore, T samples showed the maximum mean crushing load of 57.59 kN together with a good repeatability and stable crush response. It was seen that the initial peak and mean crushing loads were increased when the location of cut-outs was getting closer to the top portion of samples. This can be attributed to the beginning of progressive end crushing after the cut-outs line. For a reliable evaluation of loading characteristics, crushing load efficiency, which is shown in Fig. 9b, should be examined carefully. T samples had the maximum load efficiency, with the value of 80.98%, in the crushing process due to the close position of cut-outs behaved like a trigger mechanism that provides a progressive crushing process initiating the collapsing [19].

The energy absorption values of the samples for different cut-out locations are shown in Fig. 10. The maximum values as 3145.86 J and 45.47 J/g in terms of total and specific energy absorption, respectively, were obtained from T samples. These values were 23.5% and 19.44% higher than that of C samples. With respect to the crashworthiness performance of T samples, it can be expressed that circular cut-outs should be used as possible as closed to crushed ends in order to obtain a stable crush process resulted with higher energy absorption. This can also be minimized the casualties by reducing the acceleration experienced by passengers.
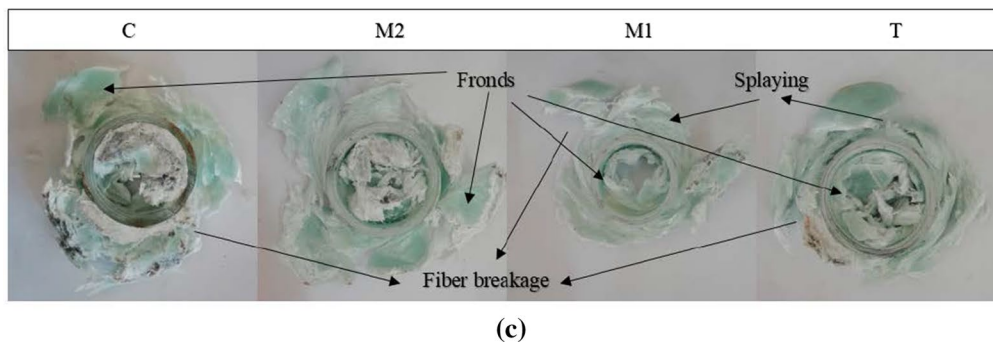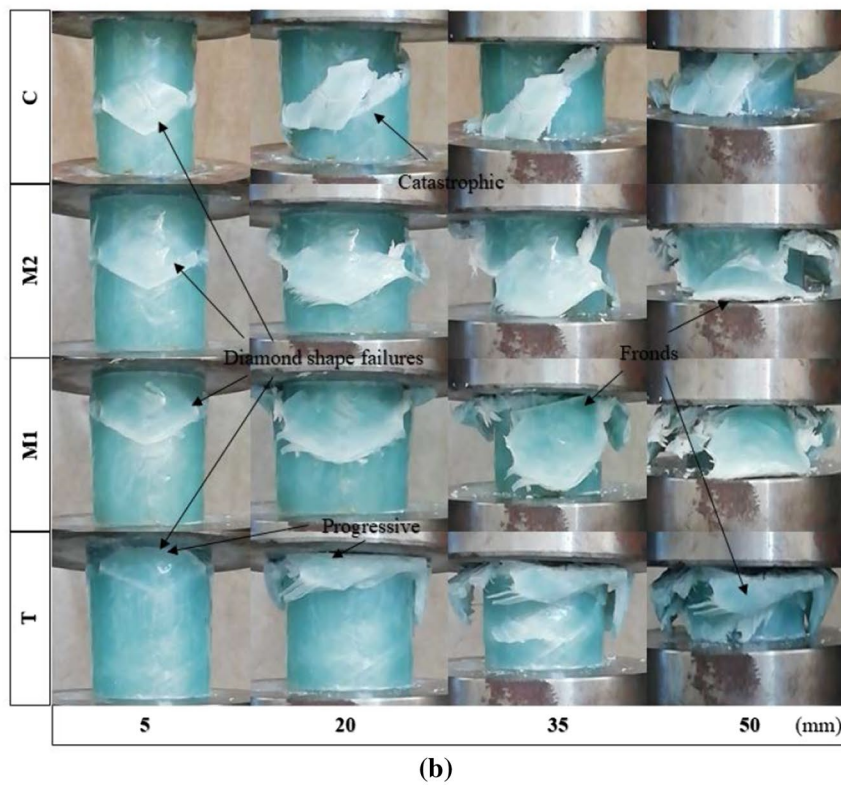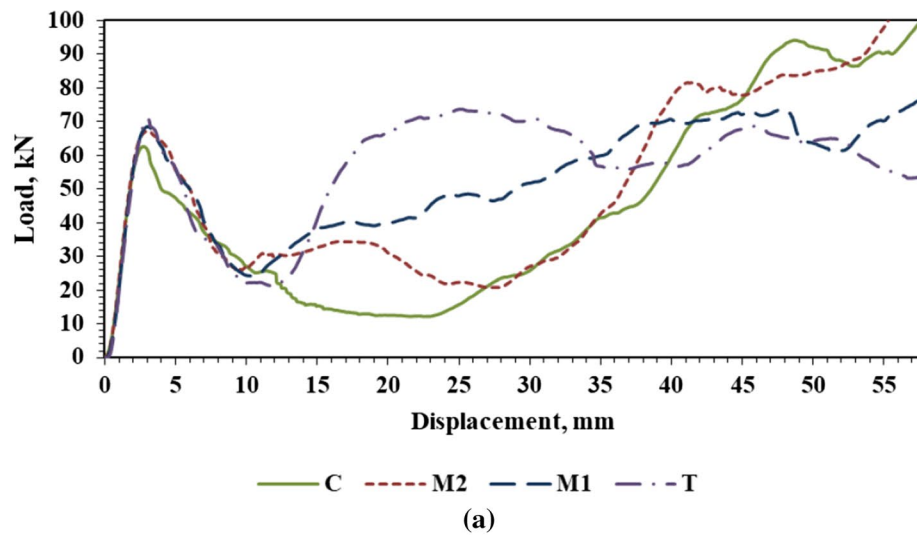
(a)

(b)

(c)

Fig. 8 GFRP samples with the various location of cut-outs; **a** load–displacement response, **b** crush history, **c** after experiments
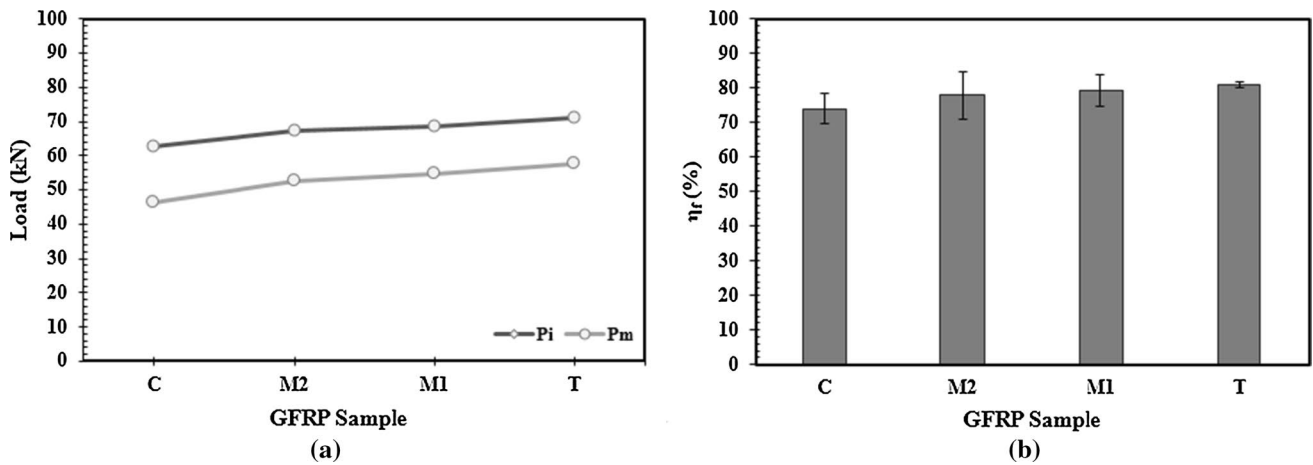
Fig. 9 Loading characteristics for different locations of cut-outs; **a** initial peak and mean loads, **b** crushing load efficiency
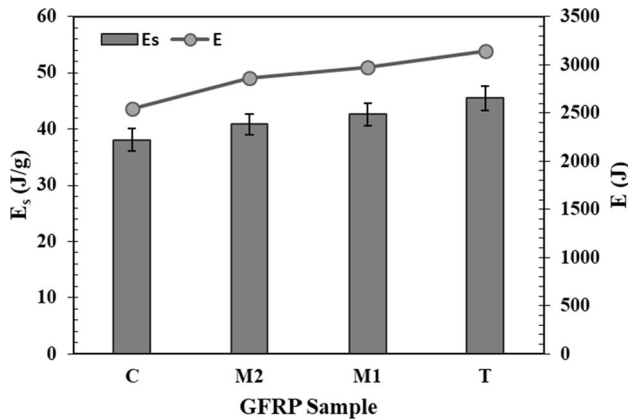
Fig. 10 Energy absorption for different locations of cut-outs

3.3 Size of cut-outs

As can be seen from the previous sections, having three circular cut-outs at the top of the sample is seemed as the most efficient configuration for a crushing application among the cases studied. In this section of the study, the influence of size or diameter of circular cut-outs on crashworthiness performance was analyzed. Till here, cut-outs with 10 mm diameter properly as suggested formulation by Toda [55] were used. Herein, the diameters of 4, 6, 8, 12, and 14 mm were studied and compared with the previous results.

The crush load–displacement responses of the samples having circular cut-outs in different sizes are presented in Fig. 11. Due to the different sizes had no significant effects on the failure modes and crushing histories that were achieved with T samples, they were not given here. Even though the load response of all samples showed a rapid drop after the elastic region, the load immediately increased and

Fig. 11 Load–displacement curves of GFRP samples with different sizes of cut-outs
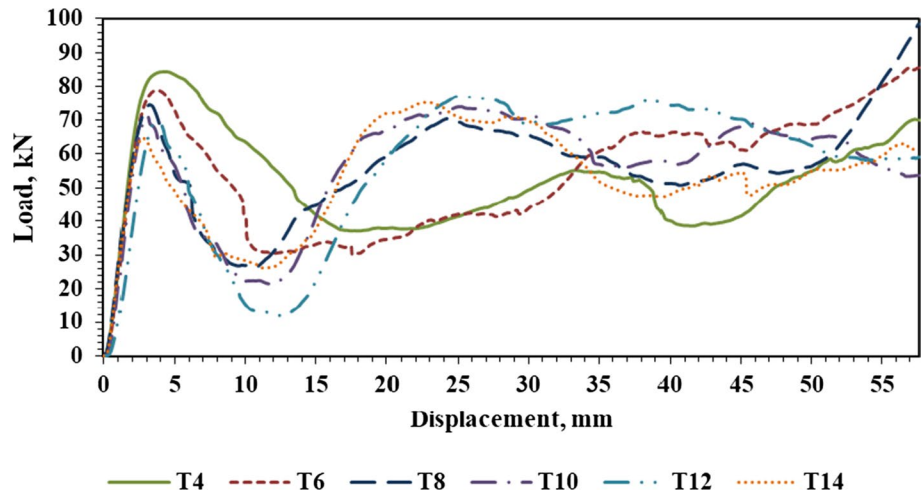
becomes stable during the crushing stage. The main reason for this was the cut-outs exhibited behavior like a trigger mechanism that stabilizes the crushing process leading to rapid decreases in loads at beginning of the post-crushing stage [5]. Additionally, it can be said that the load-bearing capability of the samples was decreased with an increment in size. However, a different scenario was obtained from the crushing area which was the part after the elastic region. Even they looked like a more stable curve, it was obvious that T4 and T6 samples had the lower load-carrying capacity of crushing whole the curve response. While other samples exhibited dramatic decreases after initial peak points, early sharp increases resulted with higher crushing load responses. In general, all samples exhibiting a stable curve and good reproducibility showed progressive crush process. The major energy absorption was contributed from the axial cracking and matrix fragmentations for all samples [5].

The loading characteristics of the GFRP samples with different sizes of cut-outs in terms of initial peak load mean crushing load, and crushing load efficiency are presented in Fig. 12. It was clear that as the diameter of the cut-out increased, decreases in initial peak load and increases in mean crushing load were obtained [19]. The initial peak load and mean crushing load which protecting the gap between them were seen as the stable lines around T10 and T12. Even though T14 samples showed a close relationship that resulted with higher crushing load efficiency, the load-bearing capability should be considered for preventing the material weakness. Until T10, there was a big gap that may the catastrophic failures in crushing response of materials. The maximum initial peak and mean crushing loads were obtained from T10 samples as 71.11 kN and 57.59 kN, respectively. Besides, T12 samples with the highest crushing load efficiency of 83.76% had 3.4% more than T10 samples. It can be said that the higher size of cut-outs showed increases in load efficiency due to lower

load-bearing capability or initial peak loads in the elastic region that comes from early failures.

The energy absorption results of the samples are given in Fig. 13. From the failure responses and loading characteristics, T10 and T12 samples received great attention among all configurations having different sizes. Here, it was observed that an increasing trend with an increment of the diameter values up to T10, while larger sizes had a decreasing tendency. This was consistent with that the higher size of cut-out holes resulted with decreases in initial peak loads [19]. T10 samples exhibiting the best energy absorption capability both of the total and specific can be chosen as the best configuration.

4 Summary of the cut-out design

The crashworthiness indicators for all GFRP pipe series are given in Table 2. For the number of cut-outs, 3 cut-outs (C3) exhibited the highest values except for the initial peak load.
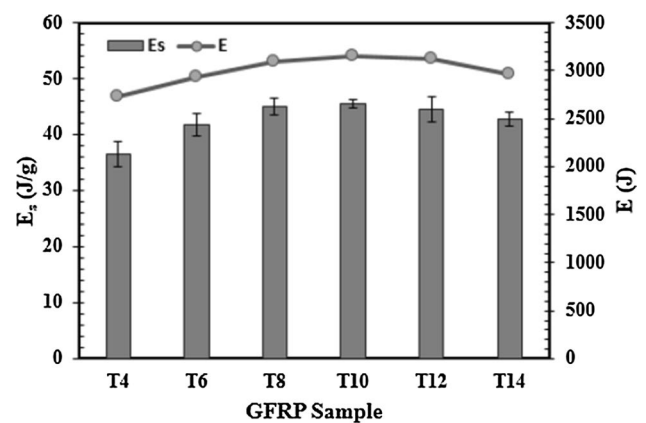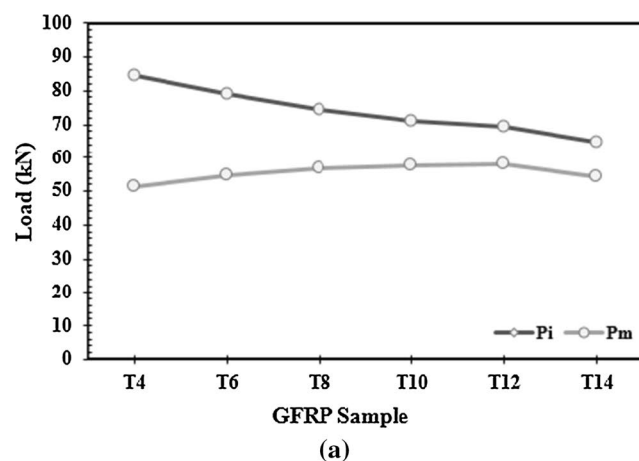

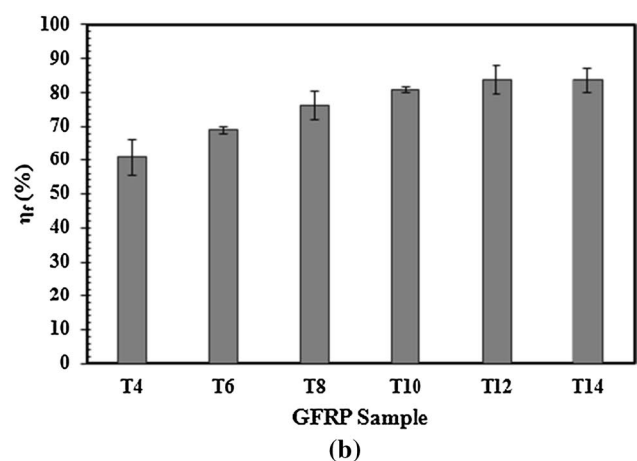**Fig. 13** Energy absorption for different locations of cut-outs

Fig. 12 Loading characteristics for different locations of cut-outs; **a** initial peak and mean loads, **b** crushing load efficiency

Table 2 Summary of the crashworthiness parameters of all GFRP pipe series

GFRP sample	P_{mean} (N)	P_i (N)	η_f (%)	m_{crush} (g)	E (J)	E_s (J/g)
C0	38,628.50	75,215.62	51.36	66.35	2102.03	31.68
C2	44,908.26	65,393.36	68.67	66.85	2458.73	36.78
C3/C	46,372.16	62,622.02	74.05	66.89	2546.60	38.07
C4	36,031.64	61,909.96	58.20	65.61	1975.73	30.11
M2	52,524.93	67,394.98	77.94	70.14	2864.80	40.85
M1	54,468.89	68,703.03	79.28	69.74	2973.09	42.63
T/T10	57,590.11	71,114.82	80.98	69.18	3145.86	45.47
T4	51,293.62	84,443.28	60.74	74.72	2733.52	36.58
T6	54,442.03	78,893.56	69.01	70.19	2933.06	41.79
T8	56,737.23	74,516.16	76.14	68.46	3087.45	45.10
T12	58,011.51	69,258.69	83.76	70.24	3125.37	44.49
T14	54,045.81	64,584.92	83.68	69.28	2968.02	42.84

From the location of cut-out, the closer position of cut-outs to the impacted end of the pipe samples (T) was seen as the best configuration exhibiting maximum performance for all parameters. Also, as the diameter of the cut-out increased, higher crushing load efficiency and lower initial peak load were achieved. However, the energy absorption characteristics of GFRP samples which are the most important criteria in a crash event were getting poor. So, the samples with 10 mm diameter (T10) were chosen as the optimum configuration among these results. The results of study can be helpful for the design and potential use of filament wound composite structures in engineering applications that exposed to crush loading such as transport vehicles, z-struts of commercial aircraft fuselage structures.

5 Conclusions

In this study, the circular cut-outs were studied to develop a trigger mechanism in the composite pipes subjected to quasi-static axial compression loading in a crash event. The composite pipes made of glass/epoxy with $\pm(55°)_6$ fiber orientation were fabricated by the wet filament winding technique. The number, location and size of the circular cut-outs were considered as the design parameters for the trigger mechanism to be examined. According to their failure response, loading characteristics, and energy absorption, the pipe samples having 3 circular cut-outs were showed the better results than the samples having 0, 2 and 4 circular cut-outs in the first group that deals with the number of circular cut-outs. In the examination of cut-out locations, the closer position of cut-outs to the impacted end of the pipe samples (T) was exhibited the maximum performance for all parameters. Increment in the diameter of the cut-outs was resulted with the increase in efficiency and decrease in initial peak load; however, these led to poor energy absorption characteristics which is the

most important criteria in a crash event. Although they could not the highest values for loading characteristics, the samples with 10 mm size and three circular cut-outs at the closer location to the top end of the pipes exhibiting the higher values in terms of load-bearing capability and energy absorption were evaluated as the best configuration among the examined cases for crashworthiness behaviors of GFRP samples. These results showed that crashworthiness performance of GFRP samples can be improved with the trigger mechanisms to be formed with the appropriate implementation of circular cut-outs.

References

1. World Health Organization (2018) Global status report on road safety 2018: summary (No. WHO/NMH/NVI/18.20). World Health Organization
2. Ferdynus M, Rozylo P, Rogala M (2020) Energy absorption capability of thin-walled prismatic aluminum tubes with spherical indentations. Materials 13(19):4304
3. Ren Y, Jiang H, Liu Z (2019) Evaluation of double-and triple-coupled triggering mechanisms to improve crashworthiness of composite tubes. Int J Mech Sci 157:1–12
4. Zhang T, Liu TG, Xiao HL, Yu XF (2006) Energy absorption performance of thin-walled structures with triggering holes subjected to high-speed axial impact. Explosion Shock Waves 26(5):395
5. Yuen S, Nurick GN (2008) The energy-absorbing characteristics of tubular structures with geometric and material modifications: an overview. Appl Mech Rev 61(2)
6. Song HW, Du XW, Zhao GF (2002) Energy absorption behavior of double-chamfer triggered glass/epoxy circular tubes. J Compos Mater 36(18):2183–2198
7. Tong Y, Xu Y (2018) Improvement of crash energy absorption of 2D braided composite tubes through an innovative chamfer external triggers. Int J Impact Eng 111:11–20
8. Siromani D, Henderson G, Mikita D, Mirarchi K, Park R, Smolko J, Awerbuch J, Tan TM (2014) An experimental study on the effect of failure trigger mechanisms on the energy absorption capability of CFRP tubes under axial compression. Compos A Appl Sci Manuf 64:25–35

9. Jiang H, Ren Y (2019) Crashworthiness and failure analysis of steeple-triggered hat-shaped composite structure under the axial and oblique crushing load. Compos Struct 229:111375
10. Liu H, Falzon BG, Dear JP (2019) An experimental and numerical study on the crush behaviour of hybrid unidirectional/woven carbon-fibre reinforced composite laminates. Int J Mech Sci 164:105160
11. Flesher ND, Chang FK, Janapala NR, Starbuck JM (2011) A dynamic crash model for energy absorption in braided composite materials-Part II: Implementation and verification. J Compos Mater 45(8):867–882
12. Eshkoor RA, Oshkovr SA, Sulong AB, Zulkifli R, Ariffin AK, Azhari CH (2013) Effect of trigger configuration on the crashworthiness characteristics of natural silk epoxy composite tubes. Compos B Eng 55:5–10
13. Huang JC, Wang XW (2010) Effect of the SMA trigger on the energy absorption characteristics of CFRP circular tubes. J Compos Mater 44(5):639–651
14. Joosten MW, Dutton S, Kelly D, Thomson R (2010) Experimental evaluation of the crush energy absorption of triggered composite sandwich panels under quasi-static edgewise compressive loading. Compos A Appl Sci Manuf 41(9):1099–1106
15. Kindervater CM, Johnson AF, Kohlgrüber D, Lützenburger M, Pentecote N (2000) Crash and impact simulation of aircraft structures-hybrid and FE based approaches. In: European congress on computational methods in applied sciences and engineering. Barcelona, Spain: ECCOMAS
16. Jahani M, Beheshti H, Heidari-Rarani M (2019) Effects of geometry, triggering and foam-filling on crashworthiness behaviour of a cylindrical composite crash box. Int J Automotive Mech Eng 16(2):6568–6587
17. Käfer B, Bheemineni VK, Lammer H, Kotnik M, Riemelmoser FO (2013) Effects of position and cut-out lengths on the axial crushing behavior of aluminum tubes: experimental and simulation. Int J Civ Environ Eng 7(11):2157–2164
18. Chiu YS, Jenq ST (2014) Crushing behavior of metallic thin-wall tubes with triggering mechanisms due to quasi-static axial compression. J Chin Inst Eng 37(4):469–478
19. Rai V, Ghasemnejad H, Watson JW, Gonzalez-Domingo JA, Webb PF (2019) Developed trigger mechanisms to improve crush force efficiency of aluminium tubes. Eng Struct 199:109620
20. Mamalis AG, Manolakos DE, Ioannidis MB, Papapostolou DP (2005) On the crushing response of composite sandwich panels subjected to edgewise compression: experimental. Compos Struct 71(2):246–257
21. Palanivelu S, Van Paepegem W, Degrieck J, Van Ackeren J, Kakogiannis D, Van Hemelrijck D, Wastiels J, Vantomme J (2010) Experimental study on the axial crushing behaviour of pultruded composite tubes. Polym Testing 29(2):224–234
22. Özbek Ö, Bozkurt ÖY (2019) Hoop tensile and compression behavior of glass-carbon intraply hybrid fiber reinforced filament wound composite pipes. Mater Testing 61(8):763–769
23. Özkılıç YO, Yazman Ş, Aksoylu C, Arslan MH, Gemi L (2021) Numerical investigation of the parameters influencing the behavior of dapped end prefabricated concrete purlins with and without CFRP strengthening. Construct Build Mater 275:122173
24. Bulut M (2017) Mechanical characterization of Basalt/epoxy composite laminates containing graphene nanopellets. Compos B Eng 122:71–78
25. Madenci E, Özkılıç, YO, Gemi L (2020) Buckling and free vibration analyses of pultruded GFRP laminated composites: Experimental, numerical and analytical investigations. Compos Struct 254:112806
26. Uslu E, Gavgali M, Erdal MO, Yazman Ş, Gemi L (2021) Determination of mechanical properties of polymer matrix composites reinforced with electrospinning N66, PAN, PVA and PVC nanofibers: a comparative study. Mater Today Commun 26:101939
27. Özbek Ö, Bozkurt ÖY, Erkliğ A (2021) Effect of basalt intraply fiber hybridization on the compression behavior of filament wound composite pipes. Int Polym Proc 36(2):193–204
28. Oguz ZA, Erklig A, Bozkurt ÖY (2020) Degradation of hybrid aramid/glass/epoxy composites hydrothermally aged in distilled water. J Compos Mater 0021998320984237
29. Gemi DS, Şahin ÖS, Gemi L (2021) Experimental investigation of the effect of diameter upon low velocity impact response of glass fiber reinforced composite pipes. Compos Struct 114428
30. Maziz A, Tarfaoui M, Gemi L, Rechak S, Nachtane M (2021) A progressive damage model for pressurized filament-wound hybrid composite pipe under low-velocity impact. Compos Struct 114520
31. Gemi L, Madenci E, Özkılıç YO (2021) Experimental, analytical and numerical investigation of pultruded GFRP composite beams infilled with hybrid FRP reinforced concrete. Eng Struct 244:112790
32. Oğuz ZA, Erkliğ A, Bozkurt ÖY (2021) Effects of hydrothermal seawater aging on the mechanical properties and water absorption of glass/aramid/epoxy hybrid composites. Int Polym Proc 36(1):79–93
33. Chiu LN, Falzon BG, Ruan D, Xu S, Thomson RS, Chen B, Yan W (2015) Crush responses of composite cylinder under quasi-static and dynamic loading. Compos Struct 131:90–98
34. Tan W, Falzon BG, Price M (2015) Predicting the crushing behaviour of composite material using high-fidelity finite element modelling. Int J Crashworthiness 20(1):60–77
35. Özbek Ö, Bozkurt ÖY, Erkliğ A (2019) An experimental study on intraply fiber hybridization of filament wound composite pipes subjected to quasi-static compression loading. Polym Testing 79:106082
36. Farley GL, Jones RM (1992) Crushing characteristics of continuous fiber-reinforced composite tubes. J Compos Mater 26(1):37–50
37. Cui Z, Liu Q, Sun Y, Li Q (2020) On crushing responses of filament winding CFRP/aluminum and GFRP/CFRP/aluminum hybrid structures. Compos Part B Eng 200:108341. Kompozit crush
38. McGregor C, Vaziri R, Poursartip A, Xiao X (2016) Axial crushing of triaxially braided composite tubes at quasi-static and dynamic rates. Compos Struct 157:197–206. Kompozit crush
39. Özbek Ö, Doğan NF, Bozkurt ÖY (2020) An experimental investigation on lateral crushing response of glass/carbon intraply hybrid filament wound composite pipes. J Braz Soc Mech Sci Eng 42(7):1–13
40. Wang Y, Feng J, Wu J, Hu D (2016) Effects of fiber orientation and wall thickness on energy absorption characteristics of carbon-reinforced composite tubes under different loading conditions. Compos Struct 153:356–368
41. Roslan MN, Yahya MY, Ahmad Z, Abdul Rashid AH, Wang WX (2018) Energy absorption capacity of basalt sandwich composite cylinder subjected to axial compression loadings. In: Materials science forum (vol 917, pp 7–11). Trans Tech Publications Ltd
42. Elgalai AM, Mahdi E, Hamouda AMS, Sahari BS (2004) Crushing response of composite corrugated tubes to quasi-static axial loading. Compos Struct 66(1–4):665–671
43. Liu Q, Xing H, Ju Y, Ou Z, Li Q (2014) Quasi-static axial crushing and transverse bending of double hat shaped CFRP tubes. Compos Struct 117:1–11
44. Hu D, Zhang C, Ma X, Song B (2016) Effect of fiber orientation on energy absorption characteristics of glass cloth/epoxy composite tubes under axial quasi-static and impact crushing condition. Compos A Appl Sci Manuf 90:489–501
45. Sivagurunathan R, Way SLT, Sivagurunathan L, Yaakob MY (2018) Effects of triggering mechanisms on the crashworthiness

characteristics of square woven jute/epoxy composite tubes. J Reinf Plast Compos 37(12):824–840

46. Jimenez MA, Miravete A, Larrode E, Revuelta D (2000) Effect of trigger geometry on energy absorption in composite profiles. Compos Struct 48(1–3):107–111

47. Song Z, Ming S, Li T, Du K, Zhou C, Wang B Improving the energy absorption capacity of square CFRP tubes with cutout by introducing chamfer. Int J Mech Sci 189:105994

48. Huang J, Wang X (2010) On a new crush trigger for energy absorption of composite tubes. Int J Crashworthiness 15(6):625–634

49. Peters ST (ed) (2011) Composite filament winding. ASM International

50. ASTM D2584 (2002) Standard test method for ignition loss of cured reinforced resins. In: American Society for Testing and Materials (vol 100)

51. Ramakrishna S, Hamada H (1998) Energy absorption characteristics of crash worthy structural composite materials. In: Key engineering materials (vol 141, pp 585–622). Trans Tech Publications Ltd

52. Palanivelu S, Van Paepegem W, Degrieck J, Vantomme J, Kakogiannis D, Van Ackeren J, Van Hemelrijck D, Wastiels J (2011) Crushing and energy absorption performance of different geometrical shapes of small-scale glass/polyester composite tubes under quasi-static loading conditions. Compos Struct 93(2):992–1007

53. Gupta NK, Gupta SK (1993) Effect of annealing, size and cutouts on axial collapse behaviour of circular tubes. Int J Mech Sci 35(7):597–613

54. Zhang XW, Tian QD, Yu TX (2009) Axial crushing of circular tubes with buckling initiators. Thin-walled Struct 47(6–7):788–797

55. Toda S (1983) Buckling of cylinders with cutouts under axial compression. Exp Mech 23(4):414–417